Motor Control, 1999, 3, 394-413

Identification of Time-Varying Stiffness, Damping, and Equilibrium Position in Human Forearm Movements

Jürgen Konczak, Kai Brommann, and Karl Theodor Kalveram

Knowledge of how stiffness, damping, and the equilibrium position of specific limbs change during voluntary motion is important for understanding basic strategies of neuromotor control. Presented here is an algorithm for identifying time-dependent changes in joint stiffness, damping, and equilibrium position of the human forearm. The procedure requires data from only a single trial. The method relies neither on an analysis of the resonant frequency of the arm nor on the presence of an external bias force. Its validity was tested with a simulated forward model of the human forearm. Using the parameter estimations as forward model input, the angular kinematics (model output) were reconstructed and compared to the empirically measured data. Identification of mechanical impedance is based on a least-squares solution of the model equation. As a regularization technique and to improve the temporal resolution of the identification process, a moving temporal window with a variable width was imposed. The method's performance was tested by (a) identifying a priori known hypothetical time-series of stiffness, damping, and equilibrium position, and (b) determining impedance parameters from recorded single-joint forearm movements during a hold and a goal-directed movement task. The method reliably reconstructed the original angular kinematics of the artificial and human data with an average positional error of less than 0.05 rad for movement amplitudes of up to 0.9 rad, and did not yield hypermetric trajectories like previous procedures not accounting for damping.

Key Words: arm, dynamics, inverse motor models, mass-spring systems

Joint stiffness, equilibrium position, damping, and inertia are limb properties that determine the torque required to generate voluntary movements. Conversely, if an external perturbation is applied, the magnitude of the above physical parameters affects the resulting movement amplitude and velocity of the perturbed limb. Given that the inertia of a limb segment remains constant throughout a movement—this assumption is only valid for single-joint motion—joint stiffness (or its opposite, compliance), damping, and the equilibrium position of the limb

The authors are with the Department of Psychology, Motor Control Unit, Heinrich-Heine-Universität Düsseldorf, Universitätsstr. 1, Geb. 23.03, 40225 Düsseldorf, Germany.

are parameters that the nervous system can potentially manipulate through specific muscular enervation patterns.

This insight is not new and stimulated the formulation of the equilibrium theory of motor control 30 years ago (Feldman, 1966). The basic premise of this theory is that the motor control system specifies joint stiffness and equilibrium position (Latash, 1992). However, this control scheme assumes that inertia remains constant and the effect of damping is negligible for large portions of the movement. Regardless of whether one subscribes to equilibrium forms of control, the determination of how damping and stiffness properties change during voluntary movements is necessary in order to understand the operation of a neural system that controls peripheral mechanics. (We define damping as a resistive force proportional to velocity. Here the term damping is not used to denote dissipation of energy, nor should it be confused with viscosity.)

There have been many attempts to determine joint stiffness and damping based either on analysis of the resonant frequency of the limb or on recorded kinematic data following or during a mechanical perturbation (Bennett et al., 1992; De Serres & Milner, 1991; Hunter & Kearney, 1982; Kearney & Hunter, 1982; Lacquaniti et al., 1982; Latash & Gottlieb, 1991; Milner & Cloutier, 1993; Weiss et al., 1988). The proposed algorithms were able to identify the physical parameters of the limb under investigation. However, these procedures relied on ensemble methods. That is, identification was based on averaging several "similar" movement trials with the average movement being subtracted from the perturbed motion. The temporal resolution of the identification methods was rather coarse, wherein the identified parameters were either constants, changed monotonically (Lacquaniti et al., 1982), or could only be identified reliably over at least half a movement cycle (De Serres & Milner, 1991). Most methods estimated inertia, stiffness, and damping; other procedures yielded time-varying equilibrium positions and stiffness coefficients of the arm, yet did not consider temporal changes in damping (Latash & Gottlieb, 1991).

The limitations of ensemble methods were recently overcome by Xu and Hollerbach (1998), who presented a method for estimating time-varying compliance parameters from a single movement. Relying on a randomly varying bias torque generated by an airjet propulsion actuator, their procedure estimates inertia, stiffness, and damping, but not the equilibrium position. While the above studies were restricted to single-joint movements, Gomi and Kawato (1997) studied two-joint arm movements and identified the corresponding stiffness and damping matrix. They found that equilibrium and actual trajectories had similar shapes, but the actual and predicted velocity profiles were quite different, leading them to conclude that the brain also takes limb dynamics into account.

The estimation of physical parameters like stiffness and damping coefficients is an ill-posed problem violating at least one of the three Hadamard conditions: existence, uniqueness, stability of the solution. Small errors in the kinematic data (i.e., noise, time delays) will lead to large errors in the estimated variables (Kalveram & Natke, 1997). Possible countermeasures against this problem are regularization methods like statistical weighting within the estimation procedure (Natke, 1992). We employed such a regularization technique by designing an estimation algorithm with a moving window.

The purpose of this paper is to present a method for identifying the time-varying mechanical parameters of a single limb. We set out to accomplish two

goals: First, to determine time-dependent changes in joint stiffness, damping, and equilibrium position in human forearm movements based on data of a single movement. The validity of the parameter estimations is checked by comparing the originally recorded kinematics with the angular kinematics obtained by a forward model that receives the estimated limb parameters as input. Second, to implement a procedure that does not rely on the analysis of the resonant limb frequency or the presence of an external mechanical perturbation to yield reasonable results.

Method

Experimental Apparatus

The type of movements under investigation were flexion-extension of the human forearm around the elbow joint. We used a similar experimental setup as described by Milner and Cloutier (1993). Subjects put their arm into an orthosis that was attached to the upper lever of a manipulandum (see Figure 1). Movements of upper and lower lever were coupled by two flatirons. External mechanical perturbations to the arm-lever system were generated by a torque motor whose shaft was rigidly connected to the lower lever. The power amplifier driving the torque motor received its input from an Eltec TE 84/68 K computer. A strain gauge on one flatiron measured the torque applied by the subject to the motor shaft. In addition, a potentiometer and tachometer coupled to the motor shaft measured angular position and velocity of the two levers.

Subjects and Procedure

We recorded single-joint elbow movements of 6 subjects, ages 23 to 57 years. Their body weight ranged between 63 and 85 kg. None had any record of a neurological motor disorder. The results of the identification procedure were rather similar across subjects. For the sake of brevity, we only present individual data from 3 subjects. However, our conclusions and our experience with the proposed identification algorithm are based on the complete sample.

Subjects viewed their current endpoint position and the required target position on a convex screen about 1.5 m in front of them. Both positions were indicated by two illuminated arrows pointing toward each other. We recorded movements during two conditions: a *hold* task and a *movement* task. In the hold task, subjects had to maintain an elbow position of 90° flexion. After 2 seconds, a short 100-ms force pulse was applied, generating a flexor torque of 2.6 Nm. Subjects were instructed not to cocontract their arm muscles prior to the perturbation in order to fixate the forearm. However, with the onset of the perturbation the subjects were to return the arm as quickly as possible to its original position. We collected electromyography from three arm muscles—M. biceps brachii, triceps brachii, and brachioradialis—to examine whether subjects did relax their arm muscles prior to the perturbation. In the second task, subjects had to perform a goal-directed elbow flexion movement to a specified target. Movement amplitude was 50°. No external torque pulses perturbed arm motion during these trials.

All kinematic and EMG data were sampled at 520 Hz and digitized with a 12-bit analog-to-digital converter (Burr-Brown MPV904). Subsequently, the angular kinematic data were low-pass filtered with a 12-Hz recursive 4th-order Butterworth filter. Based on the angular position signal, we derived angular velocity and acceleration.

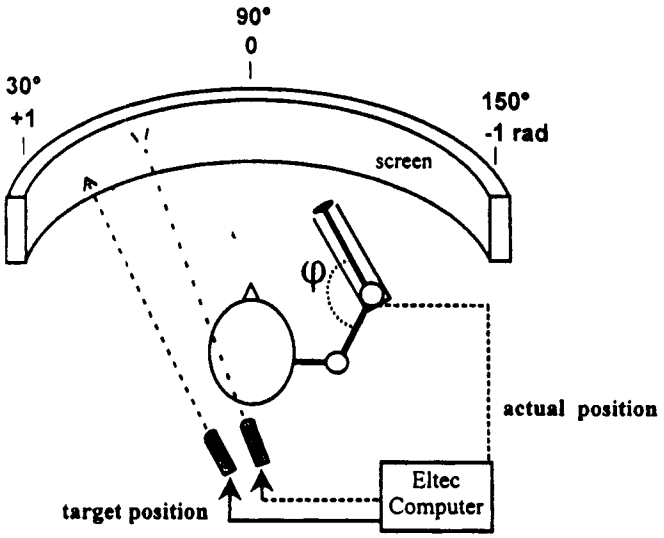

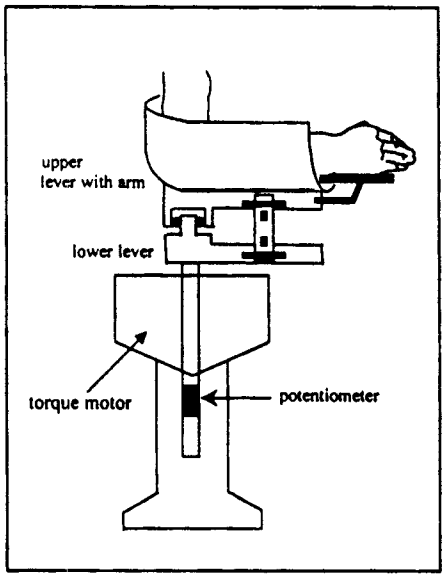

Figure 1 — Experimental apparatus. Two rotating flashlights projected the arm's current endpoint position and the required target position on a convex screen about 1.5 m in front of the subject. Positions were indicated by two illuminated arrows pointing toward each other. In our setup, an elbow angle φ of 90° corresponds to a 0 rad position on the screen, −1 rad to an elbow position of 147°. Increasing φ translates into elbow flexion, a decreasing angle into joint extension.

Estimation of Inertia

Prior to the experiment, the inertial coefficient of the experimental apparatus (J_{lever}) without the human arm inserted was determined. This was achieved by applying a known stiffness K via the torque-motor, displacing the lever from its resting position, and recording the resulting kinematics upon release of the lever until the lever came to a halt. Subsequently, the inertia of the lever was computed to be 0.096 kgm² based on its resonant frequency. The angular moment of inertia of the human arm (J_{human}) for each subject was calculated by using an anthropometric model (Clauser et al., 1969; Dempster, 1955). For the 6 subjects the values for J_{human} ranged between 0.074 and 0.139 kgm². For comparison, Bennett et al. (1992) reported a mean value of 0.072 kgm², while Latash and Gottlieb (1991) estimated inertia to 0.102 kgm² for their group.

Model of the Experimental Setup

The mechanical behavior of the human forearm with the manipulandum that is exposed to an external perturbation can be modeled by the standard differential equation for a dampened harmonic oscillator.

$$T(t) = J\ddot{\varphi} + B(t)\,\dot{\varphi} + K(t)\,(\varphi - \varphi_0(t)) \tag{1}$$

where φ, $\dot{\varphi}$, and $\ddot{\varphi}$ are *angular position, velocity, and acceleration*.

The coefficients J, $B(t)$, and $K(t)$ represent total inertia, total damping, and total stiffness of the arm-lever system, and $\varphi_0(t)$ is the equilibrium position of the arm system (limb + lever). The subscript (t) indicates that a particular parameter is time-dependent. The moment of inertia J is constant over time. $T(t)$ is the external torque applied by the motor.

Parameter Identification

For the second step, the actual identification procedure, we transformed Equation 1:

$$T(t) - J\ddot{\varphi}(t) = B(t)\,\dot{\varphi} + K(t)\,\varphi(t) - K(t)\,\varphi_0(t) \cdot 1 \tag{2}$$

To obtain estimates for $B(t)$, $K(t)$, and $\varphi_0(t)$, we used a method of solving linear equations that had been proposed previously (e.g., Kalveram, 1992; Latash, 1993). In order to solve for $B(t)$, $K(t)$, and $-K(t)\,\varphi_0(t)$, we rewrote Equation 2:

$$\begin{bmatrix} T(t) - J\,\ddot{\varphi}(t) \\ \cdot \\ \cdot \\ \cdot \end{bmatrix} = \begin{bmatrix} \dot{\varphi}(t) & \varphi(t) & 1 \\ \cdot & \cdot & \cdot \\ \cdot & \cdot & \cdot \\ \cdot & \cdot & \cdot \end{bmatrix} \begin{bmatrix} B(t) \\ K(t) \\ -K(t)\,\varphi_0(t) \end{bmatrix} \tag{3}$$

$T(t)$ and $\varphi(t)$ with its derivatives are values measured at successive points in time. Equation 3 represents an overdetermined system of linear nonhomogeneous equations, with $B(t)$, $K(t)$, and $-K(t)\,\varphi_0(t)$ as unknowns, and angular position, velocity, and 1 as coefficients. If the rank of the matrix of coefficients is 3, a solution to Equation 3 can be obtained on the basis of 3 consecutive samples of the angular kinematics and the applied motor torque. In practice, however, the rank

can be lower than 3 (ill-conditioned matrix) and the data of just 3 timed samples will not suffice. In this case, solving for $B(t)$, $K(t)$, and $\varphi_0(t)$ becomes an ill-posed problem. That is, an infinite number of possible solutions does exist.

To address the problem and to obtain parameter estimations that change over time, we designed a moving window algorithm. The size of the window could assume a value between a minimum of 3 samples and a maximum of all recorded samples of a given trial. However, if the window is too small, the identified parameter time-series become discontinuous, and the subsequent kinematic reconstruction will fail. On the other hand, if the selected window is too large, then the identification is essentially an averaging procedure over a long time period.

While a kinematic reconstruction with constant parameters for large portions of the movement is possible, we found that this does not produce a good fit with respect to the originally recorded data. Hence we applied two criteria for selecting a specific window size: First, the resulting parameter estimation should yield a continuous time series. Second, the estimation should provide the reconstructed kinematics whereby the root mean square error (RMS error) with respect to the original recorded kinematics is minimized. Selected is the smallest window that fulfills both criteria. For identifying the center-hold task with movement times of up to 2 seconds, we found that a window size of 201 data points (≈388 ms) fulfilled the above criteria, while for fast ramp-like movements, window sizes of 41–61 data points (≈77–118 ms) yielded the smallest error in the kinematic reconstruction (see Table 1).

Similar to a moving-average procedure, the specified window moved for each time increment (here: 0.0019 s) from the beginning to the end of the data matrix of Equation 3. On the basis of the data within the window, the parameter estimation was performed for each data step, with the value of the estimated parameter being in the exact middle of the window. Effectively, this moving-window algorithm performs like a digital filter leading to solutions with low-frequency changes in each of the three identified parameters.

In order to achieve physiologically plausible results, we set further restrictions: First, stiffness $K(t)$ had to assume a positive value (there is no physiological

Table 1 Changes in RMS Error as a Function of Window Size

Window size samples [ms]	Error		
	Postion [rad]	Velocity [rad/s]	Acceleration [rad/s²]
181 (310)	0.0040	0.0789	2.356
201 (348)	**0.0037**	**0.0757**	**2.367**
221 (387)	0.0039	0.0765	2.396
241 (425)	0.0044	0.0802	2.457

Note: Based on a single trial during the hold task. Continuity (1st selection criterion) was obtained at window size value of 181 (first row). Identification with a window size of 201 provided the smallest error in angular position and velocity (2nd selection criterion).

or physical evidence for negative joint stiffness). Second, values of the equilibrium position had to stay within the boundaries of the range of motion of the elbow joint (in theory the equilibrium position can be specified outside the range of motion).

Results

Parameter Identification

Simulation Data. A general problem when estimating parameters of mechanical impedance from human data is that the true time-dependent changes of damping, stiffness, and equilibrium position of the limb are not known. Thus it is difficult to decide whether the identification technique employed actually yields a reasonable solution. To validate our method, we decided to resort to artificial data created with appropriate software (MatLab). First we generated vectors of $T(t)$, $B(t)$, $K(t)$, and $\varphi_0(t)$. Next, these vectors were used as input to a computer simulation, modeling the arm-lever system described by Equations 4 and 5 (see Appendix). The output of the model was a set of angular kinematics $\varphi(t)$, $d\varphi/dt$, $d^2\varphi/dt^2$). We used as simulation software Simulink (Math Works, Inc.). The following parameters were preset prior to the start of simulation: (a) Stiffness of the steel flatirons, connecting upper and lower lever K_s = 100,000 Nm/rad; (b) Inertia of the lower lever J_{lever} = 0.096 kgm², and inertia of the upper lever including the human arm J_{human} = 0.08 kgm². At simulation time t=0, the equilibrium position was –0.1 rad, the actual arm position was 0.6 rad (in our experimental setup an elbow angle of 90° corresponded to 0 rad; see Figure 1). Step rate of the simulation was 520 Hz, which was the same sampling rate for collecting the human data in our setup. Subsequently, we used total inertia ($J_{lever} + J_{human}$), $T(t)$ and the simulated angular kinematics ($\varphi(t)$, $d\varphi/dt$, $d^2\varphi/dt^2$) as input to our identification routine.

Thus, we could compare the original parameters of $B(t)$, $K(t)$, and $\varphi_0(t)$ with the estimated parameters derived from our identification procedure. As seen in Figure 2, the time-dependent parameters $B(t)$, $K(t)$, and $\varphi_0(t)$ were identified with reasonable accuracy. RMS errors of the estimated parameters with respect to the original values were: $\varphi_{0,\,ide}$ = 0.05 rad, B_{ide} = 0.2 Nm/rad/s, K_{ide}= 2 Nm/rad. Finally, we assessed whether the identified parameters were suitable for reconstructing the original kinematics. The identified parameters $B(t)$, $K(t)$, and $\varphi_0(t)$ were inserted into our model of the experimental setup (arm + lever + motor) and the simulation was repeated using the same starting conditions as described above. The resulting angular kinematics were then compared to the original kinematic data. Figure 3 reveals that the original and reconstructed angular position correspond closely, indicating that the differences between the original and re-identified values of B, K, and φ_0 were marginal. That is, the formal solution found by our identification procedure resembled closely the time-course of the actual values of B, K, and φ_0 and changed slowly below 2 Hz. The procedure also yielded unique solutions when B, K, and φ_0 changed at frequencies exceeding 2 Hz. However, in these cases the reconstructed and original kinematics could differ substantially.

Human Data: Hold Task. After validating our method with simulated data, we applied it to human data. Subjects performed a perturbation task. While holding their forearms at 90° flexion, an external torque pulse of 100 ms duration was applied. They were instructed to reassume the previous position as fast as possible after perturbation. The identified parameters for K, B, and φ_0 are shown Figure 4.

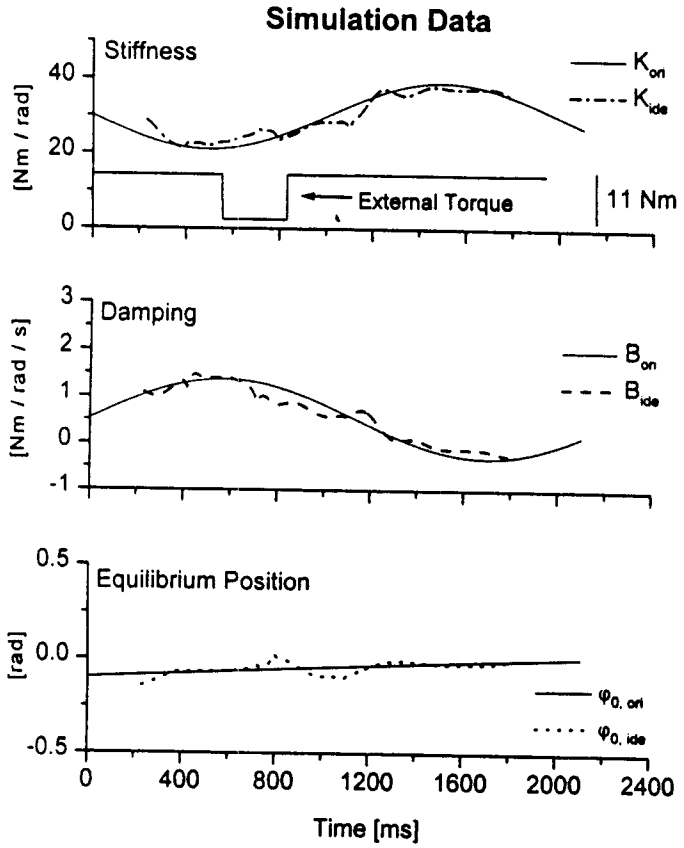

Figure 2 — Simulation data. Re-identification of artificially generated time-varying parameters of stiffness (K_{on}), damping (B_{on}), and equilibrium position ($\varphi_{0,\,on}$). The corresponding estimated parameters are K_{ide}, B_{ide}, $\varphi_{0,\,ide}$. Top graph also shows simulated external torque (T). Window size of the identification was set to 201 data points (= 387 ms).

In this trial, joint stiffness and damping were kept constant for most of the movement time. Both parameters increased only during the final breaking phase. The equilibrium position of the arm (φ_0) basically remained at 0 rad (90° elbow flexion). Following the same procedure we used for the artificial data, the identified parameter values of B, K, and φ_0 were inserted into the forearm simulation. The resulting reconstructed kinematics closely resembled the recorded kinematics, indicating that a valid solution was found (Figure 5).

Figure 6 reveals how the inertial, resistive, and stiffness related torque components of the above trial change over time. The values are based on the estimated parameters presented in Figure 4. The torque-time data in Figure 6 demonstrate the different contributions of each torque component during the various phases of the movement. The initial external torque pulse (T) extended the forearm from its resting position at 90° elbow flexion. Subsequently, stiffness related torque, K

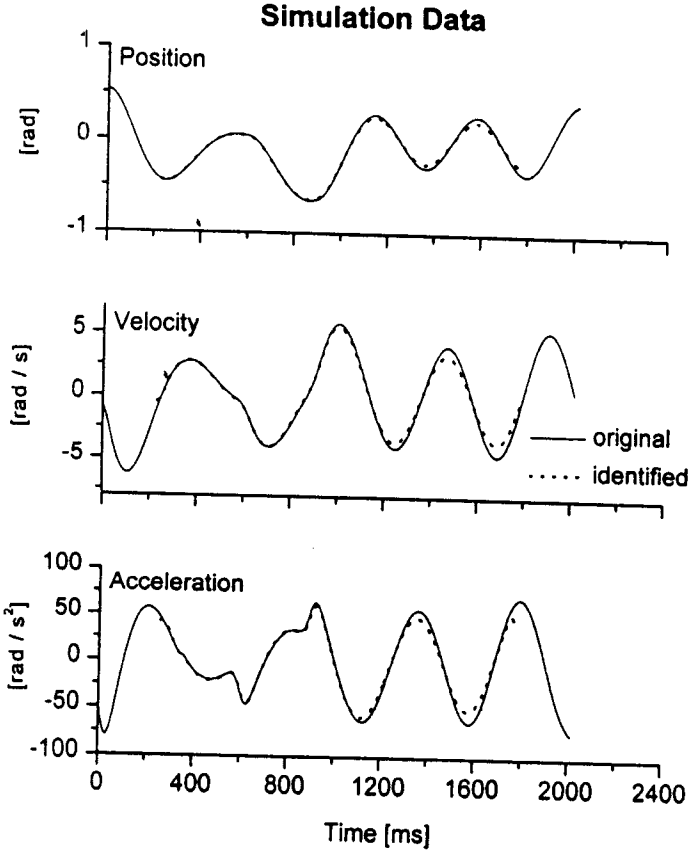

Figure 3 — Simulation data. Reconstruction of angular kinematics based on identified parameters K_{ide}, B_{ide}, and $\varphi_{0,\,ide}$. (Parameters correspond to data in Figure 2). *Original* refers to angular kinematic time-series that were used as input to the identification procedure. *Identified* curves are the reconstructed kinematics based on parameter estimation. RMS errors of reconstructed kinematics with respect to original data were: position (0.03 rad), velocity (0.4 rad/s), acceleration (7 rad/s²).

$(\varphi-\varphi_0)$, became the major torque to counterbalance the inertial effects ($J\, d^2\varphi/d^2t$), while resistive torques ($B\, d\varphi/dt$) were especially prominent as breaking forces at the end of the movement.

Comparing Different Approaches. Next we tested how different system identification models could reconstruct the recorded angular kinematics. Figure 7 shows the obtained angular positions under: (a) a full model, where $B(t)$, $K(t)$, and $\varphi_0(t)$ were determined; (b) a reduced model that does not account for the damping component, i.e., only $K(t)$ and $\varphi_0(t)$ were identified; and (c) a simplified model, where $B(t)$ was set to 0 after parameter identification. Considering the various torque components in Figure 6, it seems obvious that setting an identified time-series of $B(t)$ to 0 should produce characteristic positional errors especially at the

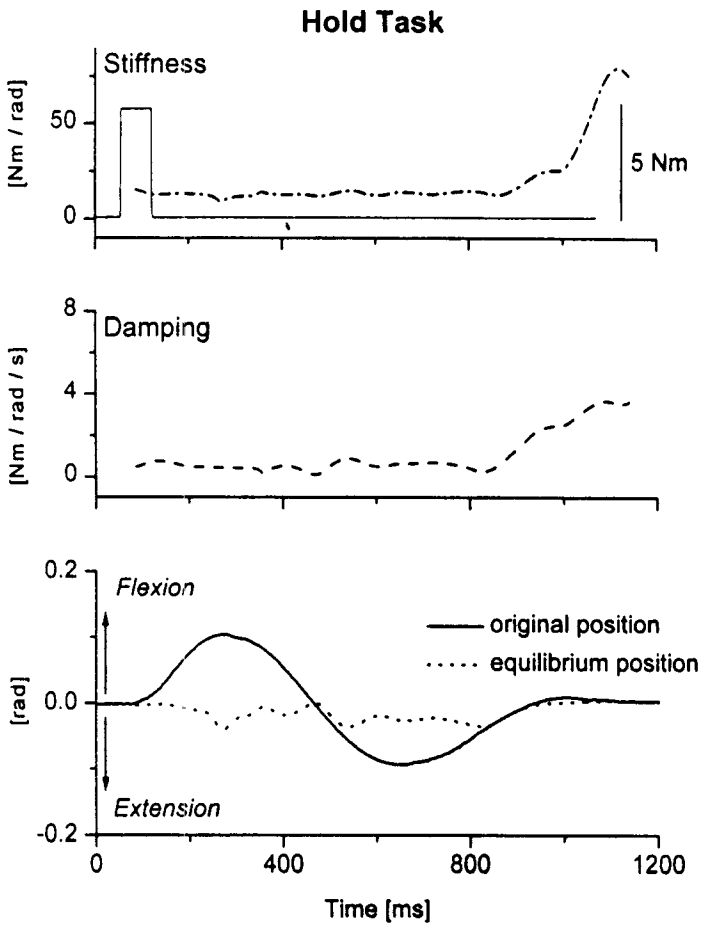

Figure 4 — Hold task. Identification of human elbow joint stiffness, damping, and equilibrium position. The subject was instructed to maintain a center position (0 rad angle) and return to this position as fast as possible after external perturbation. Top graph also shows the exerted motor torque (T). In the bottom graph, *original position* refers to actual recorded angular position of forearm. Window size was set to 201 data points (= 387 ms).

end of the movement. However, a similar trend was also found for the position curve derived from the reduced model. Both position time-series were hypermetric when compared to the originally recorded $\varphi(t)$. Figure 7 demonstrates that only the full model accounting for the resistive torque component could reproduce the position trajectory at movement termination with reasonable accuracy.

Human Data: Movement Task. Subjects were instructed to perform a 50° elbow flexion, starting from an initial elbow angle of 120°. Movements were performed under the presence of a constant extensor torque of 1.4 Nm, or without the

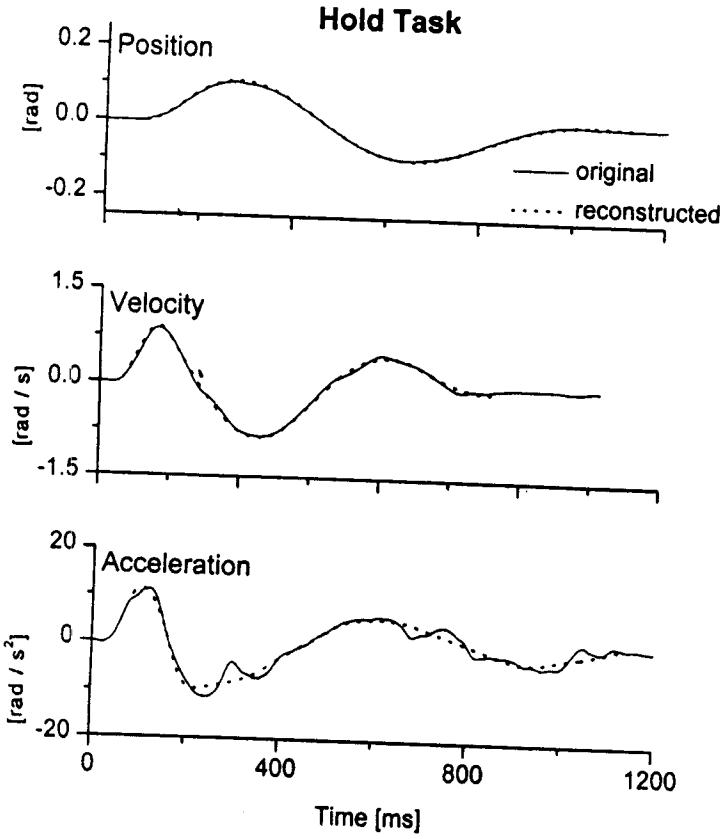

Figure 5 — Hold task. Reconstruction of angular kinematics based on parameter estimation of K, B, and φ_0. Data correspond to the identified parameters in Figure 4. Top graph presents original and reconstructed angular position of forearm. The two bottom graphs show the respective angular velocity and acceleration. RMS errors of the reconstructed kinematics with respect to original data were: position (0.002 rad), velocity (0.033 rad/s), acceleration (1.1 rad/s²).

presence of any bias torque. No external torque pulses were applied to perturb the arm during execution. In general, the parameter estimations were not reliable for the first 200–250 ms after movement onset due to lack of information in the data prior to movement start (angular kinematics were nearly constant). Thus, for the parameter estimation right after movement onset, the estimation window still contains kinematic data with little or no movement at all. Consequently, the identification procedure cannot be very reliable for those initial intervals. The resulting sharp drops in K_{ide}, and the negative values for B_{ide} that are seen especially at movement start, are an artefact of the method and are not interpretable.

Figure 8 shows the time-varying changes in equilibrium position stiffness when performing a single voluntary elbow flexion. During the movement, damping and stiffness increased almost linearly as they did during the hold task. In

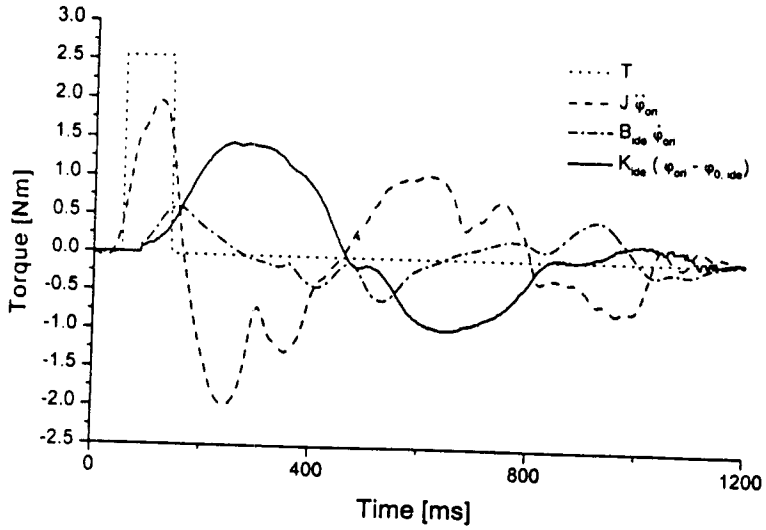

Figure 6 — Hold task. Time-varying contributions of various torque components based on parameter estimations of J, B, and K. Shown are the torque generated by the motor (dotted), inertial torque (dashed), damping related torque (dash-dot), and stiffness related torque (solid). It appears here that acceleration is increasing before the external torque T rises, but this was not the case. The effect is an artefact due to the application of the Butterworth filter.

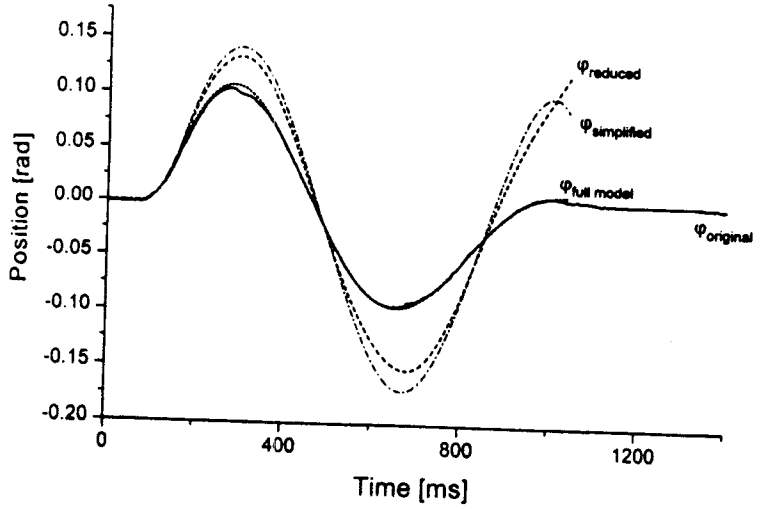

Figure 7 — Hold task. Effects of different identification models on reconstructing the observed angular position. The curve ($\varphi_{simplified}$) results if damping is set to 0 in a full model. The curve $\varphi_{reduced}$ results if a reduced model is used that disregards the effect of damping. Implementing a full model ($\varphi_{full\ model}$) yields a curve that most closely resembles the recorded angular position data ($\varphi_{original}$).

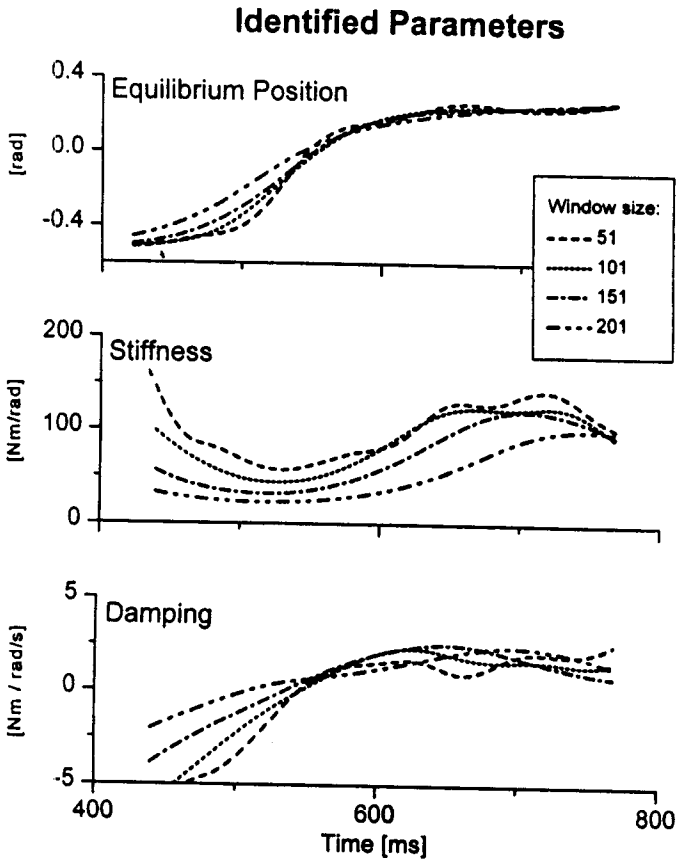

Figure 8 — Movement task. Identification of human elbow joint stiffness, damping, and equilibrium position using different window sizes. The subject was instructed to perform a 45° elbow flexion to a specified target. No force pulse was applied during the movement. Window size values correspond to number of samples within the window. Samples were collected every 1.9 ms. Time scale reflects the actual recording time. Movement started about 380 ms after beginning of recording.

contrast to the hold task, the equilibrium position changes drastically after movement onset, describing an s-shaped trajectory. The s-shape trajectory could transform into an N-shape trajectory for very fast movements, similar to the trajectories reported by Latash and Gottlieb (1991).

The data in Figure 8 also indicate the effect of the selected window size on the estimation of the mechanical parameters. The three graphs show that the selection of another window does not result in drastically different time series of damping, stiffness, and equilibrium position. Increasing the size of the window basically leads to smoother trajectories. Yet, as demonstrated in Figure 9, the tradeoff of selecting a larger window size is an inferior kinematic reconstruction with a larger error.

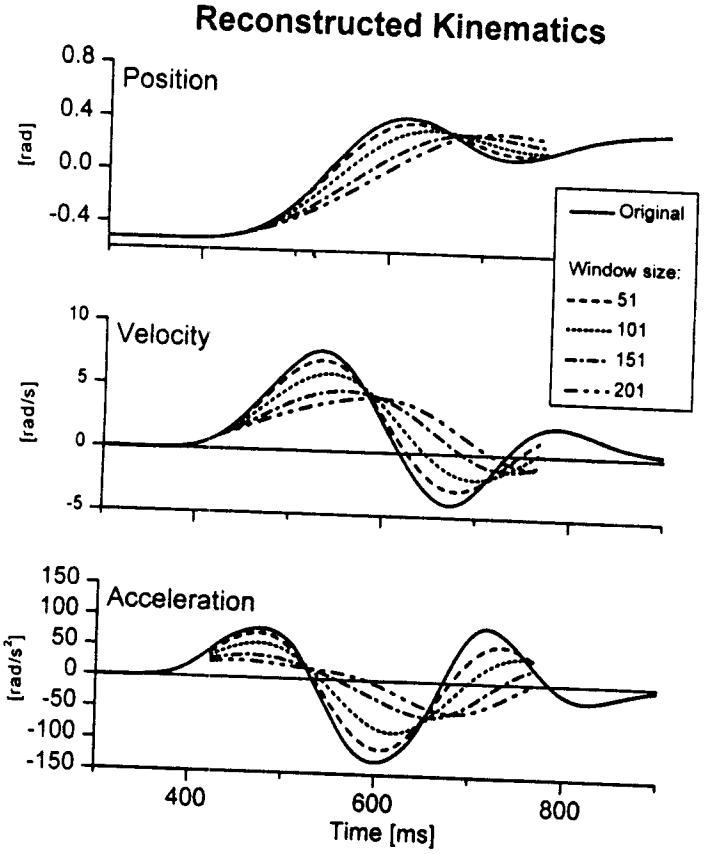

Figure 9 — Movement task. Reconstruction of angular kinematics based on the identified parameters of K, B, and φ_0 shown in Figure 8. Top graph presents original and reconstructed angular position of forearm, the two bottom graphs the angular velocity and acceleration. *Original* refers to actual recorded angular position of the forearm. Note that selecting a larger window during identification leads to smoother kinematic trajectories, which result in larger deviations between original and reconstructed kinematics.

Next we investigated the consistency of the parameter identification across several trials by letting subjects perform repeated trials with varying movement amplitudes. Exemplar for this data set, Figure 10 shows the variability of the parameter estimation for 5 consecutive trials. The subject performed 45° forearm flexion movements with no external torque present during execution. Similar to the data shown in Figure 8, stiffness was basically constant at the beginning of the movement and increased until the end of the movement. Damping increased monotonically. Again, a caveat about the validity of data at the beginning (negative damping) and end of the movement is warranted. Toward the beginning and end of

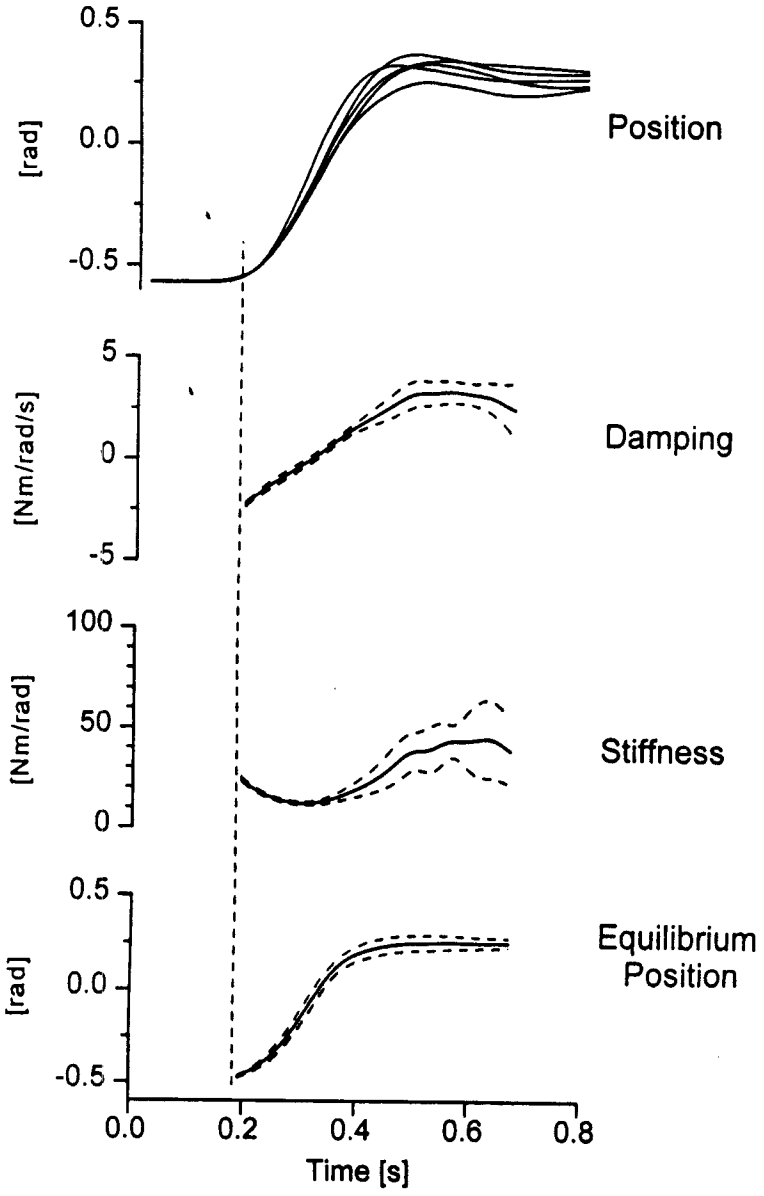

Figure 10 — Movement task. Parameter estimation for 5 consecutive 45° elbow flexion movements of one subject. Top graph shows individual angular trajectories illustrating the degree of between-trial variability. The three bottom graphs show mean (solid line) and corresponding standard deviation (dashed line) of each estimated parameter. These time-series are clipped at the beginning and end of each trial.

each stiffness and damping time-series, the actual values should be viewed with caution because at these times the moving window necessarily contains data with little or no motion. Note that the variability in the parameter estimations reflects the between-trial variability in the kinematic data—a repeated identification using the same widow size would result in identical parameter estimations.

With regard to goal-directed movements of different amplitudes (15, 30, 45° flexion, extension movements), we found that only equilibrium position changed as a function of amplitude. The time-series of stiffness and damping remained nearly invariant throughout the three tested movement amplitudes.

Discussion

The precise determination of the time-varying changes of damping, stiffness, and equilibrium position during voluntary movement has been an issue in motor control for the last decade (Bennett et al., 1992; Gomi & Kawato, 1997; Lacquaniti et al., 1982; Latash & Gottlieb, 1991; Milner, 1993; Xu & Hollerbach, 1998). Assuming that the physical behavior of the human arm is adequately described by a damped mass-spring model, the identification of its parameters may provide insight into the underlying processes of neural control. We here present an algorithm that can identify such mechanical parameters. The identification procedure is constrained by the assumption that these parameters vary slowly over time. This assumption seems reasonable given that (a) previous research indicated that during single-joint motion the equilibrium trajectories change monotonically or at a low frequency (Latash & Gottlieb, 1991), and (b) muscle dynamics may take on the form of a low-pass filter in simple tasks, thus preventing high-frequency changes of muscle related damping and stiffness (Zajac & Winters, 1990).[1]

Comparison to Previous Estimation Procedures

We regard our method as an extension of the earlier studies that also attempted to identify the time-dependent changes in stiffness, damping, and equilibrium position (Bennett et al., 1992; Lacquaniti et al., 1982; Milner & Cloutier 1993; Xu & Hollerbach, 1998). With the exception of Xu and Hollerbach (1998), all previous estimation procedures are ensemble methods. That is, they rely on averaging techniques across several trials. In contrast, the method proposed by Xu and Hollerbach and our own algorithm can identify parameters from single trial data. The differences between Xu and Hollerbach's model and ours is that their model does not estimate the equilibrium position (φ_0), while it is time-varying in our case. In addition, we calculated inertia prior to estimation based on anthropometric measures and inserted its known value into the model equation, while Xu and Hollerbach actually estimated inertia. We initially tried to estimate inertia in addition to the other parameters but saw that the reconstructed kinematics based on these estimations produced larger errors than our method presented here. This was especially true for movements with sinusoidal trajectories as in our hold task. In these cases,

[1]This is not to say that muscles behave like simple smoothing filters of higher frequency EMG input. In unloaded movements especially, the muscle shortens quicker than its associated force trajectory. Nonlinearities arise when more than one muscle is involved.

position and acceleration have "similar" time series, and the estimation procedure does not yield plausible results (i.e., large fluctuations in inertia). To remedy this, we opted to determine inertia based on anthropometric measures and used the calculated value of inertia for the identification routine.

Finally, note that our method does not rely on the continuous application of an external perturbation torque during motion in order to obtain estimation results that reliably reproduce the recorded kinematics (see Figure 9). However, we clearly state that the presence of an external torque can improve identification in those instances where there are little or no temporal changes in the angular kinematics (very slow movements). In those instances, the application of small irregular torques will likely improve estimation as shown in previous experiments (Gomi & Kawato, 1997; Xu & Hollerbach, 1998).

Our procedure represents a modification of the method used by Latash and Gottlieb (1991), wherein the inertia of the system is determined a priori and the damping factor B is not considered. Here we demonstrate that keeping the damping factor constant, setting it to zero, or attempting to calculate its contribution into stiffness and equilibrium position leads to hypermetric trajectories in the kinematic reconstruction (Figure 7). In the mass-spring model used, the contribution of damping cannot simply be assigned to stiffness or inertia, because position and acceleration are essentially orthogonal to velocity. Consequently, to neglect damping will provide erroneous results, especially for movements with a sinusoidal position trajectory such as in our hold task. We would argue that at least for those types of movements, a full model is more complete and provides a better fit of the observed kinematics. Assuming that a linear time varying model is appropriate, this finding points out that any neural controller needs to consider how its efferent commands affect mechanical stiffness *and* damping at the limb/joint level. However, we should realize that this assumption might be too simplistic, especially if one considers the control of multijoint movements using multiarticulate muscles.

Limitations of the Method

In fairness, our algorithm suffers from some of the same problems as previous methods. Movement phases, where position or velocity are constant, will almost always lead to insensible solutions. This is also true for episodes, where position and velocity have "similar" trajectories (i.e., both rise monotonically). In this context, we found it imperative to check the validity of the found solution by testing whether the identified parameters could reproduce the original kinematics. Further, the method is restricted to determine joint related changes. It is not suitable to make any valid statement about the stiffness and damping of the involved muscles and tendons.

In its current version, the identification procedure assumes a linear angle-torque relationship. This is not true for extreme joint positions or at high levels of tonic muscle force where stiffness declines (Sinkjaer et al., 1988). Yet ours is not a linear model in the strict sense, where B, K, and φ_0 are constants. Allowing B, K, and φ_0 to change over time introduces nonlinearity to the model. In this respect, our model represents an improvement over approaches that regard these parameters as constants. However, it could be that the true angle-torque relationship is not solely time-dependent but is also a nonlinear function of φ and φ_0.

Finally, one must be careful not to draw unjustified inferences based on the parameter estimations. The identified equilibrium trajectories are not necessarily representative of a neural plan. The results from our simulation and identification simply argue that assuming the arm behaves like a dampened mass-spring, equilibrium position provides a viable control signal for goal-directed action of a single limb. However, Bellomo and Inbar (1997) recently showed that for goal-directed movements under varying inertial loads, the reconstructed equilibrium trajectories were more complicated than the simple ramp-shaped profiles proposed by Feldman and Latash, indicating that the underlying control scheme may be more complex than a simple monotonic shift of the equilibrium trajectory as we have demonstrated with our data. Finally, and most important, Zatsiorsky (1997) pointed out that the identification of these parameters may well be feasible but they have no physical relevance. That is, they are mere mathematical abstractions and, as such, have no relevance for understanding biological motor control. On the basis of our data we cannot fully refute this argument, although we would hope, together with those researchers who have also worked on system identification, that this approach provides useful information for a better understanding of how the nervous system can control limb dynamics.

In conclusion, our method is not a "wunderkind" solving all previous reported problems of parameter estimation. Yet we believe it may present a valuable addition to the present system identification techniques. A possible extension of the procedure is the use of more complex window algorithms whereby window size is adaptable during the identification process and/or a weighting function is imposed to the data within the window.

References

Bellomo, A., & Inbar, G. (1997). Examination of the lambda equilibrium point hypothesis when applied to single degree of freedom movements performed with different inertial loads. *Biological Cybernetics*, **76**, 63-72.

Bennett, D.J., Hollerbach, J.M., Xu, Y., & Hunter, I.W. (1992). Time-varying stiffness of human elbow joint during cyclic voluntary movement. *Experimental Brain Research*, **88**, 433-442.

Clauser, C.E., McConville, J.T., & Young, J.W. (1969). *Weight, volume, and center of mass of segments of the human body* (Tech. Report No. AMRL-TR 69-70). Dayton, OH: Wright-Patterson Air Force Base.

De Serres, S.J., & Milner, T.E. (1991). Wrist muscle activation patterns and stiffness associated with stable and unstable mechanical loads. *Experimental Brain Research*, **86**, 451-458.

Dempster, W.T. (1955). *Space requirements of the seated operator* (Tech. Report No. WADC TR 55-159). Dayton, OH: Wright-Patterson Air Force Base.

Feldman, A.G. (1966). Functional tuning of the nervous system with control of movement or maintenance of a steady posture–II. Controllable parameters of the muscles. *Biofizika*, **11**, 498-508.

Gomi, H., & Kawato, M. (1997). Human arm stiffness and equilibrium-point trajectory during multi-joint movement. *Biological Cybernetics*, **76**, 163-171.

Hunter, I.W., & Kearney, R.E. (1982). Dynamics of human ankle stiffness: Variation with mean ankle torque. *Journal of Biomechanics*, **15**, 747-752.

Kalveram, K.T. (1992). A neural network model rapidly learning gains and gating of reflexes necessary to adapt to an arm's dynamics. *Biological Cybernetics*, **68**, 183-191.

Kalveram, K.T., & Natke, U. (1997). Stuttering and misguided learning of articulation and phonation, or why it is extremely difficult to measure the physical properties of limbs? In W. Hulstijn, H.F.M. Peters, & P.H.H.M. Van Lieshout (Eds.), *Speech production: Motor control, brain research and fluency disorders* (pp. 89-98). Amsterdam: Elsevier.

Kearney, R.E., & Hunter, I.W. (1982). Dynamics of human ankle stiffness: Variation with displacement amplitude. *Journal of Biomechanics*, **15**, 753-756.

Lacquaniti, F., Licata, F., & Soechting, J.F. (1982). The mechanical behavior of the human forearm in response to transient perturbations. *Biological Cybernetics*, **44**, 35-46.

Latash, M.L. (1992). Independent control of joint stiffness in the framework of the equilibrium-point hypothesis. *Biological Cybernetics*, **67**, 377-384.

Latash, M.L. (1993). *Control of human movement*. Champaign, IL: Human Kinetics.

Latash, M.L., & Gottlieb, G.L. (1991). Reconstruction of shifting elbow joint compliant characteristics during fast and slow movements. *Neuroscience*, **43**, 697-712.

Latash, M.L., & Zatsiorsky, V.M. (1993). Joint stiffness: Myth or reality? *Human Movement Science*, **12**, 653-692.

Milner, T.E. (1993). Dependence of elbow viscoelastic behavior on speed and loading in voluntary movements. *Experimental Brain Research*, **93**, 177-180.

Milner, T.E., & Cloutier, C. (1993). Compensation for mechanically unstable loading in voluntary wrist movement. *Experimental Brain Research*, **94**, 522-532.

Natke, H.G. (1992). On regularization methods within system identification. In M. Tanaka & H.D. Bui (Eds.), *Inverse problems in engineering mechanics* (pp. 3-20). Heidelberg: Springer-Verlag.

Sinkjaer, T., Toft, E., Andreassen, S., & Hornemann, B.C. (1988). Muscle stiffness in human ankle dorsiflexors: Intrinsic and reflex components. *Journal of Neurophysiology*, **60**, 1110-1121.

Weiss, P., Hunter, I.W., & Kearney, R.E. (1988). Human ankle joint stiffness over the full range of muscle activation levels. *Journal of Biomechanics*, **21**, 539-544.

Xu, Y., & Hollerbach, J.M. (1998). Identification of human joint mechanical properties from single trial data. *IEEE Transactions on Biomedical Engineering*, **45**, 1051-1060.

Zajac, F.E., & Winters, J.M. (1990). Modeling musculoskeletal movement systems: Joint and body segmental dynamics, musculoskeletal actuation, and neuromuscular control. In J.M. Winters & S.L.-Y. Woo (Eds.), *Multiple muscle systems: Biomechanics and movement organization* (pp. 121-148). New York: Springer-Verlag.

Zatsiorsky, V.M. (1997). On muscle and joint viscosity. *Motor Control*, **1**, 299-309.

Appendix

To model the mechanical behavior of the arm-lever system, we used a coupled system of two linear differential equations with nonconstant coefficients. Equation 4 represents the mechanical behavior of the upper lever with the arm inserted; Equation 5 represents the mechanics of the lower lever that is attached to the torque motor (see Figure 1).

$$T_1(t) - K_g(\varphi_1 - \varphi_2) = J_1\ddot{\varphi}_1 + B_1\dot{\varphi}_1 + K_1(\varphi_1 - \varphi_{0,1}) \qquad [\textit{upper lever \& arm}] \quad (4)$$

$$T_2(t) + K_g(\varphi_1 - \varphi_2) = J_2\ddot{\varphi}_2 + B_2\dot{\varphi}_2 \qquad [\textit{lower lever}] \quad (5)$$

$T_1(t)$: *joint torque*
$T_2(t)$: *motor torque*
$\varphi_1, \dot{\varphi}_1, \ddot{\varphi}_1$: *angular position, velocity, acceleration of upper lever & arm*
$\varphi_2, \dot{\varphi}_2, \ddot{\varphi}_2$: *angular position, velocity, acceleration of lower lever*
B_1, B_2 : *damping coefficients*
K_1 : *stiffness coefficient*
K_g : *stiffness of coupling elements (flatiron)*
J_1, J_2 : *moments of inertia*

K_g is the stiffness constant of two steel flatirons that rigidly connect the upper and lower lever of the apparatus (see Figure 1). φ_i and its derivatives represent the angular kinematics of the forearm. $\varphi_{0,i}$ refers to the equilibrium position ("zero angle") of the forearm (Latash & Zatsiorsky, 1993).

Because the two flatirons tightly coupled the motion of the upper and lower lever of the apparatus, we assume that the angular positions of the two levers are nearly identical ($\varphi_1 \approx \varphi_2$). Therefore we can simplify Equations 4 and 5 and omit the subscripts. By adding Equations 4 and 5, we obtained Equation 1.

Acknowledgment

This work was supported by grants Ka 417/18-1 and Ko 1460/8-1 of Deutsche Forschungsgemeinschaft (German Science Foundation) to K.T. Kalveram and Jürgen Konczak. We thank Sven Bestmann, Charlotte Hanisch, Marc Himmelbach, Tobias Kalenscher, Olaf Lahl, and Stefanie Richter for their invaluable help with the data collection and for programming the necessary signal processing software.

Manuscript submitted: August 31, 1998
Accepted for publication: March 1, 1999